out k space. Our procedure, consequently, attempts to approximate the distribution by a particular choice of k. A rigorous theory would consider contributions from all k, appropriately weighted.

[14]The concept of simultaneously computing scattering and dispersion is a fairly common one; cf., e.g., D. Pines and P. Nozieres, *The Theory of Quantum Liquids* (Benjamin, New York, 1966), Vol. I, p. 266.

[15]Cf., e.g., J. M. Ziman, *Principles of the Theory of Solids* (Cambridge U.P., Cambridge, England, 1964). Chap. 8.

[16]M. Born and K. Huang, in Ref. 10, Chap. II.

[17]B. Bendow, J. L. Birman, A. K. Ganguly, R. C. Leite, J. F. Scott, and T. C. Damen, Optics Commun. 1, 267 (1970).

[18]A. Messiah, in Ref. 12, p. 1005.

[19]R. Loudon, Proc. Roy. Soc. (London) A275, 218 (1963).

[20]B. Bendow, Phys. Rev. B 2, 5051 (1970).

[21]R. Loudon, J. Phys. (Paris) 26, 667 1965; and Refs. 6 and 8.

[22]Cf., e.g., J. J. Hopfield and D. G. Thomas, Phys. Rev. 132, 563 (1963).

[23]V. M. Agranovich and V. L. Ginzburg, *Spatial Dispersion in Crystal Optics and the Theory of Excitons* (Interscience, London, 1966).

[24]Cf., specifically, Eq. (4.4) in Ref. 20, which is identical with our Eq. (3.12) for Γ's = 0; also, cf. Eq. (9) of E. Burstein *et al.*, in Ref. 7.

[25]J. J. Sein, Ph.D. thesis (New York University, 1969) (unpublished); a best fit for CdS $n=1$, A-exciton data, was obtained for $\Gamma \approx 3\times10^{-4}$.

[26]R. M. Martin (private communication).

[27]J. F. Scott, R. C. Leite, and T. C. Damen, Phys. Rev. 188, 1285 (1969).

[28]R. C. Leite and S. P. Porto, Phys. Rev. Letters 17, 10 (1966); R. C. Leite and J. F. Scott, in Ref. 1.

[29]R. C. Leite, J. F. Scott, and T. C. Damen, Phys. Rev. Letters 22, 780 (1969).

[30]M. V. Klein and S. P. Porto, Phys. Rev. Letters 22, 782 (1969).

[31]S. Ushioda, A. Pinczuk, E. Burstein, and D. L. Mills, in Ref. 1.

[32]J. F. Scott *et al.*, in Ref. 1.

[33]J. M. Ralston, R. L. Wadsack, and R. K. Chang, Phys. Rev. Letters 25, 814 (1970).

PHYSICAL REVIEW B VOLUME 4, NUMBER 2 15 JULY 1971

Temperature Dependence of Vibrational Spectra in Calcite by Means of Emissivity Measurement

Takemaro Sakurai and Tsutomu Satō*
The Research Institute for Scientific Measurements, Tōhoku University, Sendai, Japan
(Received 21 December 1970)

The emissivities at various temperatures from 500 to 1200 °K, together with the reflectivity at 300 °K in calcite, were measured on the spectral region 200–4000 cm^{-1}. It was found by the measurements that conspicuous changes with temperature occurred in the reststrahlen bands of the lattice and molecular vibrations. By analyzing the reststrahlen bands, the temperature dependences of vibration parameters of the lattice vibration $E_{u(3)}$, 305 cm^{-1} in frequency, and of the molecular vibrations $A_{2u(a)}$ and $E_{u(b)}$, 886 and 1416 cm^{-1} in frequency, were obtained in the temperature range 300–1000 °K. The results were interpreted in the light of the theories on anharmonic crystals. The damping constants of the lattice and molecular vibrations were found to arise from the quartic as well as the cubic anharmonicities; the contribution of quartic anharmonicity was seen to become prominent with increasing temperatures. The frequency shifts of the lattice and molecular vibrations due to anharmonicity were found to be proportional to $-T^2$; some explanations were given for this. The oscillator strength did not show any change which exceeded the experimental error as expected theoretically.

I. INTRODUCTION

The spectral emissivity is obtained by comparing the thermal radiation of a specimen with that of a black body at the same temperature, for various frequencies. When a flat plate is used as a specimen, a theoretical calculation[1] shows that the normal emissivity ϵ is given by the following equation:

$$\epsilon = (1-T)(1-R)/(1-RT), \tag{1}$$

where T and R are transmissivity and reflectivity, respectively. In the spectral region where the transmission is very small, the above equation becomes

$$\epsilon = 1 - R, \tag{2}$$

while in the region where the reflection by specimen surfaces is very small, it becomes

$$\epsilon = 1 - T = 1 - e^{-Kd}, \tag{3}$$

where K and d are the absorption coefficient and the thickness of the specimen. Thus, the measurement of the spectral emissivity gives the optical properties of the material at elevated temperatures.

The purpose of the present work is to study the optical properties of natural calcite at elevated temperatures by means of the emissivity measurement. The infrared spectra of this material have

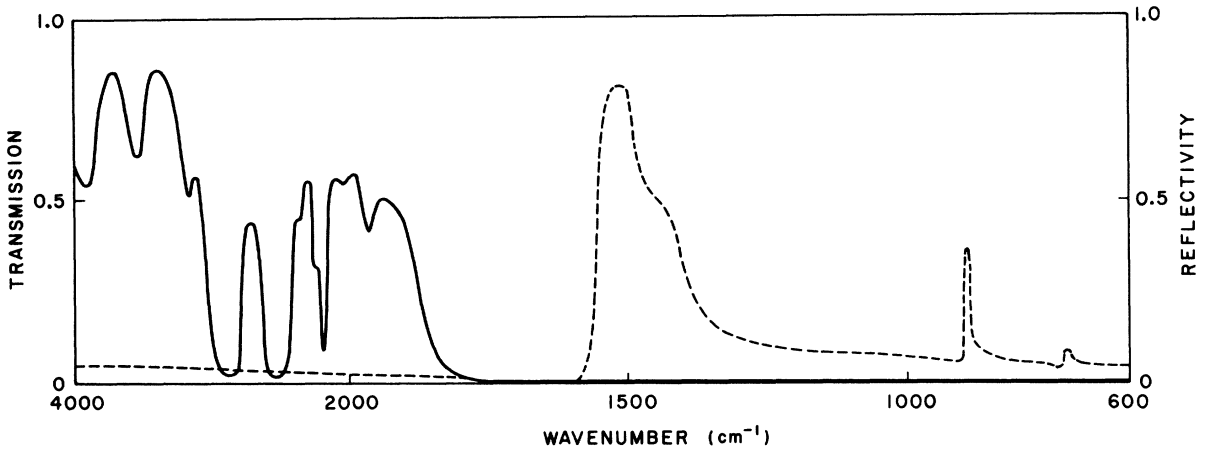

FIG. 1. Transmission (solid curve) and reflection (dotted curve) of a slab cut parallel to the rhombohedral face at 300 °K.

been investigated extensively by many workers[2–7]; those at elevated temperatures, however, have scarcely been observed. A calcite crystal has the symmetry of the space group D_{3d}^6, belonging to the trigonal system, with the rhombohedral Bravais lattice. The infrared-active modes of vibration at the zone center given by the group character analysis are illustrated in Table I, together with their hitherto assigned frequencies. The interesting point in the vibrations of this crystal is that in addition to the lattice vibrations by Ca^{++} and CO_3^{--} ions, the so-called internal or molecular vibrations by CO_3^{--} ions exist which give rise to the reststrahlen and absorption bands in the near-infrared region.

The effect of temperature on lattice vibrations was theoretically considered earlier by Born and Blackman.[8] By taking cubic anharmonicity into account, they showed that the width of the fundamental vibration increases linearly with temperature. Heilmann[9] observed the vibrational spectra of a LiF crystal at various temperatures between 300 and 900 °K and found that the damping constant changes roughly proportional to the square of the absolute temperature. Jones *et al.*[10] measured the fundamental frequency and the degree of damping at low temperatures down to 4 °K in 16 NaCl-type crystals. Similar observations were made by Woods *et al*,[11] on KBr crystal at 90 and 400 °K.

The physical properties of anharmonic crystals were further considered theoretically by several workers. Cowley and Cowley[12] treated this problem with the aid of the thermodynamic Green's function for the phonons. By using a quasiharmonic approximation, the temperature dependence of the normal mode was numerically given for NaI and KBr. More recently, Ipatova, Wallis, and Maradudin[13,14] found that the width of the fundamental lattice absorption in the high-temperature limit could be expressed by the sum of two terms, one of which is the first power and the other the second power of the absolute temperature. They gave a numerical calculation in the cases of NaCl and LiF, which showed a fair agreement with the experimental data.

Summarizing the above, it may be said that most approaches in this direction are limited to the ionic crystals of the NaCl type. Therefore, it seems worthwhile to look at the temperature dependence in crystals with other structures and to investigate what sort of dependence would appear in the molecular vibrations in the crystal. Under these considerations, the emissivity of calcite has been measured at various temperatures up to 1200 °K in the spectral region 4000–200 cm^{-1}.

II. EXPERIMENTAL PROCEDURE AND RESULTS

The crystals used in the present work were large rhombs of optical-grade calcite occurring naturally in Mexico. From these, three kinds of specimens were prepared: One of them (Rh) was a slab cleaved parallel to the rhombohedral face (1011) and

TABLE I. Infrared-active modes of vibration at the zone center and their assigned frequencies (Ref. 7). ∥ and ⊥ represent the dipole moment parallel and perpendicular to the c axis.

	E (⊥)	A_{2u} (∥)	ν (cm^{-1})
		$A_{2u(1)}$	92
Lattice vibrations	$E_{u(1)}$		102
	$E_{u(2)}$		223
	$E_{u(3)}$		297
		$A_{2u(2)}$	303
	$E_{u(a)}$		712
Molecular vibrations		$A_{2u(a)}$	872
	$E_{u(b)}$		1407

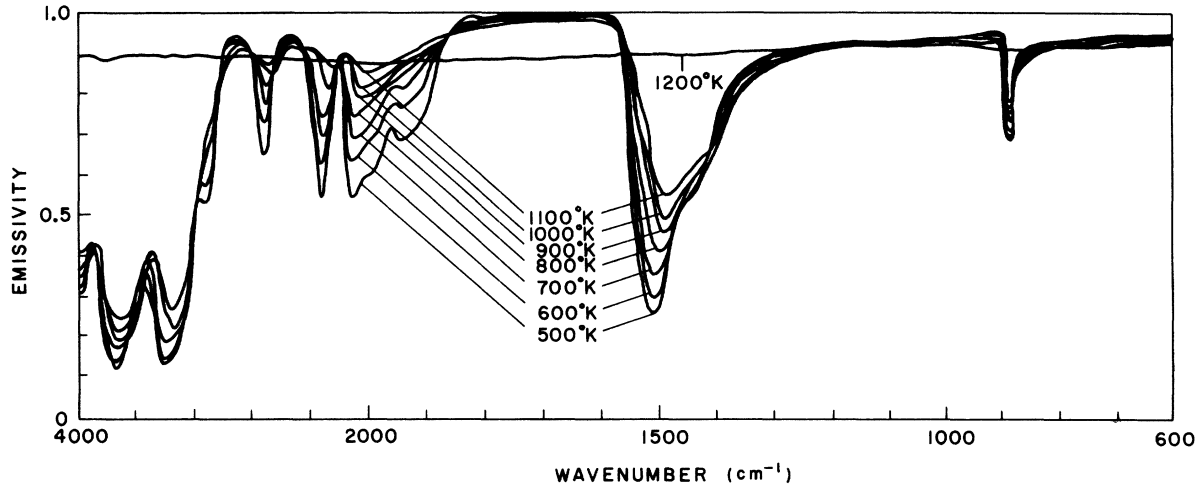

FIG. 2. Emissivities of a slab cut parallel to the rhombohedral face at various temperatures from 500 to 1200 °K.

the others, A and C, were the crystals with a surface cut parallel and perpendicular, respectively, to the crystallographic *c* axis [0001]. The surfaces were ground and polished carefully according to optical techniques to have the highest optical quality.

For measurement, a specimen and blackbody were placed at the center of an electric furnace and the thermal radiations from them were introduced into the optical paths of the sample and the reference beam in a double-beam spectrophotometer, by which the spectral emissivity of the specimen was recorded directly.

A V-shaped cavity of graphite with an emissivity of 0.97 was employed as a black body. Infrared spectrophotometers of two kinds, Japan Spectroscopic IR-S and Hitachi EPI-L, were used to cover two spectral regions, 4000–700 and 700–200 cm^{-1}, which were replaced later by a Japan Spectroscopic DS-601 because of the higher resolution.

A series of preliminary measurements were made by using cleaved specimens (Rh) 1–2 mm in thickness. The transmission and the reflectivity in the spectral region 600–4000 cm^{-1} obtained at room temperature are illustrated in Fig. 1. At frequencies higher than 1800 cm^{-1}, the specimen is partially transparent and a considerable number of summation bands appear, but it becomes perfectly opaque at lower frequencies. On the other hand, the reflectivity is very small at the frequencies above 1600 cm^{-1}, but conspicuous reststrahlen bands due to molecular vibrations appear at lower frequencies.

Using the same specimen, the emissivities were measured at various temperatures between 500 and 1200 °K. The results obtained in the region 600–4000 cm^{-1} are illustrated in Fig. 2. Comparing Figs. 1 and 2, it will be seen that the transmission minima give rise to the emissivity maxima in the partially transparent region, while the reflectivity maxima give rise to the emissivity minima in the opaque region, as are given by Eqs. (2) and (3). With increasing temperature, the summation bands are seen to show an increase in bandwidth and a slight decrease in frequency, while the reststrahlen bands are seen to show a considerable decrease in the maximum reflectivity together with a small decrease of frequency.

It is deduced theoretically that the maximum reflectivity of a reststraheln band is governed by the strength of vibration which is proportional to the number of oscillators in a unit volume and is inversely proportional to the damping constant. It is well known that when a calcite crystal is heated up to about 1100 °K it loses CO_2 and changes into CaO to make an opaque and white layer starting from the surface. Therefore, it is quite possible that the decrease of maximum reflectivity with temperature might be caused by the thermal dissociation of the reflecting surface. In order to elucidate this point, cleaved specimens were kept at the same temperature in the air for many hours and their surfaces were examined carefully; nevertheless, no change in optical qualities could be found up to 1000 °K. When the temperature was raised to 1100 °K, however, the surface showed perceptible contamination in an hour and became considerably opaque within several hours. Hence, the measurement at this temperature was finished within a fraction of an hour in order to obtain reliable data. At 1200 °K, the specimen dissociated perfectly to make a white skeleton of CaO. In the emissivity measurement, such a specimen was seen to convey radiation emitted by the wall of the furnace into a spectrophotometer by the scattering; hence, the emissivity showed a large value nearly constant throughout the whole spectral region, as exemplified in Fig. 2.

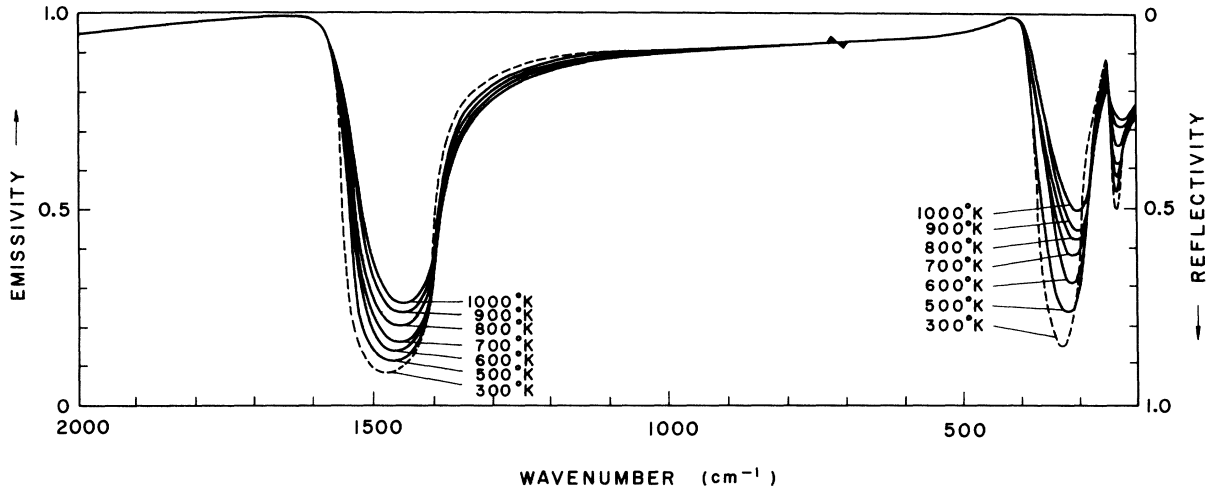

FIG. 3. Emissivities (solid curve) at various temperatures from 500 to 1000 °K and reflectivity (dotted curve) at 300 °K, obtained by a surface cut perpendicular to the c axis.

In order to observe the reststrahlen bands polarized perpendicular to the c axis separately from those polarized parallel, the finishing measurements were made by placing the (0001) face of specimen C normal to the optical axis. The emissivities obtained at various temperatures between 500 and 1000 °K in the spectral region 200–2000 cm^{-1} are illustrated by solid curves in Fig. 3, together with the reflectivity at 300 °K drawn in a dotted curve. In this figure, the reststrahlen bands of the lattice vibrations $E_{u(2)}$ and $E_{u(3)}$ and the molecular vibrations $E_{u(a)}$ and $E_{u(b)}$ appear at about 240, 330, 720, and 1500 cm^{-1}, respectively. With increasing temperature, these bands show a decrease of reflectivity and a shift towards the low-frequency side quite regularly.

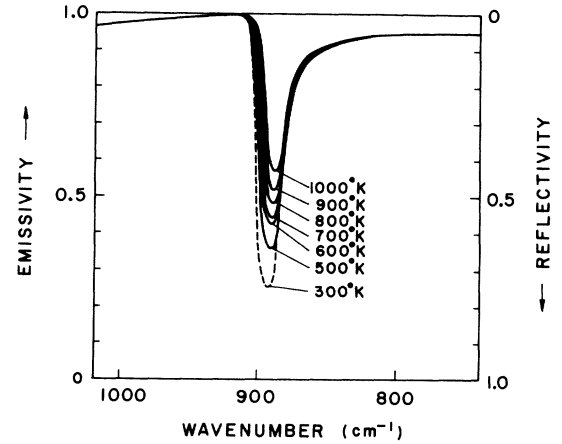

FIG. 4. Emissivities (solid curve) at various temperatures from 500 to 1000 °K and reflectivity (dotted curve) at 300 °K, obtained by a surface cut parallel to the c axis for the light polarized parallel to the c axis.

The observation of the reststrahlen bands polarized parallel to the c axis was made from the (1100) face of specimen A, eliminating the perpendicular bands by a polarizer. The emissivities of the molecular vibration $A_{2u(a)}$ with the frequency of about 890 cm^{-1} at various temperatures are reproduced in Fig. 4, which shows a similar temperature dependence, though not so conspicuous. Because of a large radiant loss due to the polarizer, the emissivity of the lattice vibration $A_{2u(2)}$ could not be given.

III. VIBRATIONAL ANALYSIS

It is clear from the results of the emissivity measurements described in Sec. II that the temperature dependence of the reststrahlen bands up to 1000 °K, to say the least, is to be ascribed not to the thermal dissociation but to some changes in the characteristics of the fundamental vibrations with temperature. Under these considerations, the observed reststrahlen bands were analysed to obtain the vibration parameters at different temperatures.

The characteristics of an individual vibration are defined by three parameters, namely, the oscillator strength $4\pi\rho_j$, the frequency ω_j, and the damping constant γ_j. The dispersion theory shows that the real and imaginary parts of the dielectric constant are represented by the following equations:

$$n^2 - k^2 = \epsilon_\infty + \sum_j \frac{4\pi\rho_j\omega_j^2(\omega_j^2 - \omega^2)}{(\omega_j^2 - \omega^2)^2 + \gamma_j^2\omega_j^2\omega^2}, \tag{4}$$

$$2nk = \sum_j \frac{4\pi\rho_j\omega_j^2\gamma_j\omega}{(\omega_j^2 - \omega^2)^2 + \gamma_j^2\omega_j^2\omega^2}, \tag{5}$$

where ϵ_∞ is the high-frequency dielectric constant, while the reflectivity R is given by the equation

$$R = [(n-1)^2 + k^2]/[(n+1)^2 + k^2]. \tag{6}$$

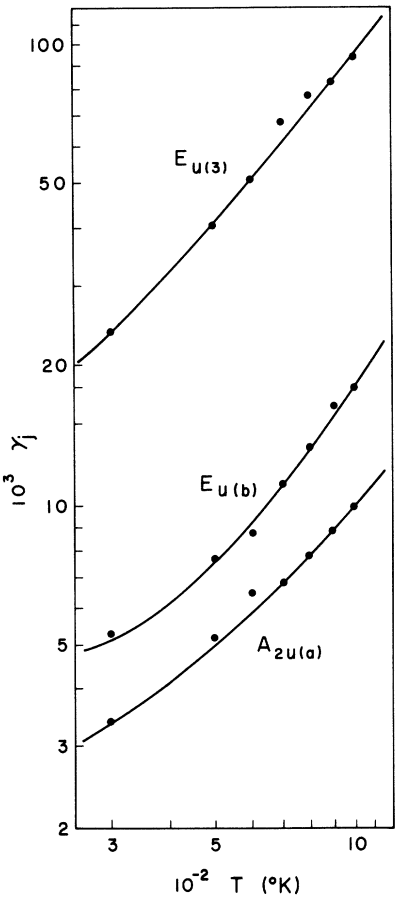

FIG. 5. Observed temperature dependence of the damping constant γ_j in the $E_{u(3)}$, $A_{2u(a)}$, and $E_{u(b)}$ modes.

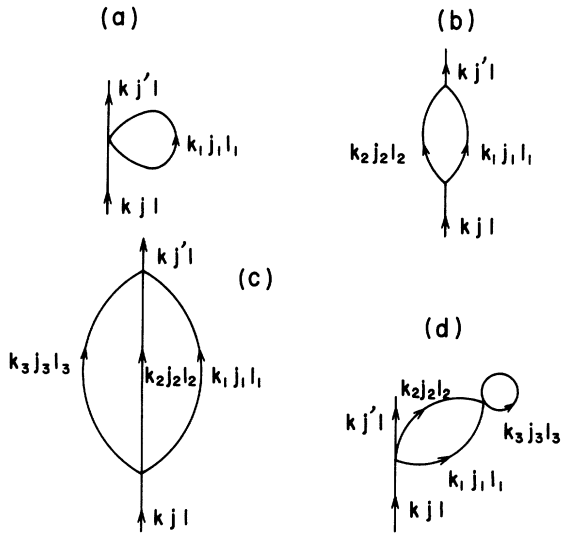

FIG. 6. Possible phonon processes arising from the anharmonicity (Ref. 13).

By using the above equations, the parameters of a series of vibrations were determined so as to ascertain the best over-all fit between the observed and calculated reststrahlen curves. The values of the parameters of the lattice vibration $E_{u(3)}$ and the molecular vibrations $A_{2u(a)}$ and $E_{u(b)}$ at various temperatures from 500 to 1000 °K obtained by analyzing the spectral emissivity are listed in Table II, together with those at 300 °K obtained by analyzing the spectral reflectivity. The parameters of other vibrations were excluded since values reliable enough to show the temperature dependence could not be obtained because of the faintness of the thermal radiation.

From the values listed in Table II, the temperature dependence of the three parameters $4\pi\rho_j$, ω_j, and γ_j can be evaluated. It will be seen in this table, first that the oscillator strength $4\pi\rho_j$ is insensitive to the temperature throughout three modes of vibration. This fact can be understood easily by seeing that the emissivity curves in Figs. 3 and 4 show an excellent agreement in the spectral regions far from the reststrahlen peaks.

On the other hand, it is known that the strength of the oscillator $4\pi\rho_j$ is expressed by the equation

$$4\pi\rho_j = 4\pi e^{*2}/VM_r\omega_j^2, \tag{7}$$

where e^* is the effective charge, V is the volume of

TABLE II. Parameters of the lattice vibration $E_{u(3)}$ and of the molecular vibrations $A_{2u(a)}$ and $E_{u(b)}$, analyzed from the observed data. The values of ϵ_∞ used in the analysis are 2.63 and 2.18 for the $E_{u(3)}$ and $A_{2u(a)}$ modes, respectively.

	$E_{u(3)}$				$A_{2u(a)}$				$E_{u(b)}$			
T (°K)	ν_j (cm^{-1})	ω_j (10^{14} sec^{-1})	$4\pi\rho_j$	γ_j (10^{-3})	ν_j (cm^{-1})	ω_j (10^{14} sec^{-1})	$4\pi\rho_j$	γ_j (10^{-3})	ν_j (cm^{-1})	ω_j (10^{14} sec^{-1})	$4\pi\rho_j$	γ_j (10^{-3})
300	305	0.575	1.40	23.8	886	1.670	0.09	3.4	1416	2.669	0.55	5.3
500	301	0.567	1.40	40.6	885	1.668	0.09	5.2	1411	2.659	0.55	7.7
600	298	0.562	1.40	51.1	885	1.668	0.09	6.5	1408	2.653	0.55	8.9
700	296	0.557	1.40	68.1	884	1.666	0.09	6.9	1403	2.645	0.55	11.3
800	291	0.549	1.40	77.8	883	1.664	0.09	7.8	1400	2.638	0.55	13.5
900	288	0.543	1.40	83.0	883	1.664	0.09	8.8	1394	2.628	0.55	16.5
1000	284	0.535	1.40	94.5	882	1.662	0.09	10.0	1390	2.620	0.55	18.1

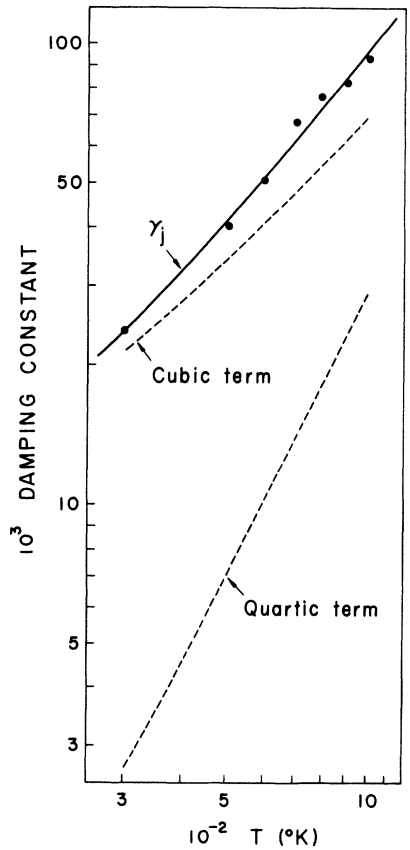

FIG. 7. Calculated curves of the cubic and quartic terms in Eq. (10) (dotted curves) and of γ_j (solid curve), and the plot of the observed values of γ_j in the $E_{u(3)}$ mode.

a primitive cell, and M_r is the reduced mass of the positive and negative ions. Therefore, it is expected that the value of $4\pi\rho_j$ will be modified by the change of V due to thermal expansion. Rao *et al.*[15] observed the thermal expansion of calcite between 273 and 524 °C and found that the coefficient of thermal expansion in the directions parallel and perpendicular to the c axis were expressed by the functions of the temperature t in °C as follows:

$$\alpha_{\parallel} = 24.670\times10^{-6} + 1.74\times10^{-8}t - 5.141\times10^{-12}t^2, \tag{8a}$$

$$\alpha_{\perp} = -3.660\times10^{-6} - 7.112\times10^{-10}t - 3.339\times10^{-12}t^2. \tag{8b}$$

TABLE III. Values of the factors a and b in Eq. (10) in the best fit with the observed values of γ_j in the $E_{u(3)}$, $A_{2u(a)}$, and $E_{u(b)}$ modes.

	a	b
$E_{u(3)}$	1.49×10^{-2}	5.96×10^{-4}
$A_{2u(a)}$	4.80×10^{-3}	3.84×10^{-4}
$E_{u(b)}$	5.21×10^{-3}	5.21×10^{-3}

With the aid of these expressions, the temperature variation of $4\pi\rho_j$ was estimated, the amount of which, however, was found not to exceed the present experimental error.

As seen in Table II, the damping constants γ_j of the three modes $E_{u(3)}$, $A_{2u(a)}$, and $E_{u(b)}$ increase conspicuously with increasing temperatures. In Fig. 5, the values of γ_j of the three modes are plotted in a logarithmic scale. The plot of the $E_{u(3)}$ mode gives a nearly linear line, the inclination of which indicates that γ_j of this mode is proportional to $T^{1.2}$. The plots of the $A_{2u(a)}$ and $E_{u(b)}$ modes, on the other hand, show slight and considerable curvatures, respectively. At high temperatures, the inclination of these curves indicates that γ_j of the $A_{2u(a)}$ mode is proportional to $T^{1.1}$ while that of the $E_{u(b)}$ is proportional to $T^{1.4}$.

It has been pointed out by Ipatova *et al.*[13,14] that the damping constant γ_j in the high-temperature limit is given as follows:

$$\gamma_j = A(T/\theta) + B(T/\theta)^2, \tag{9}$$

in which A and B are positive constants, while θ is a characteristic temperature. On the right-hand

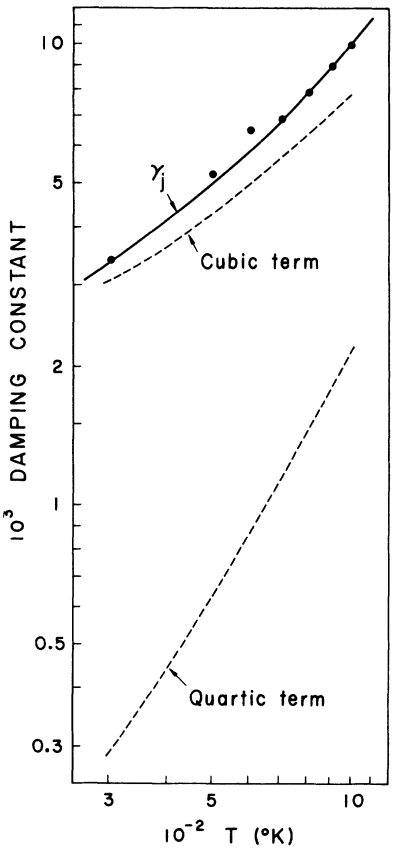

FIG. 8. Calculated curves of the cubic and quartic terms in Eq. (10) (dotted curves) and of γ_j (solid curve), and the plot of the observed values of γ_j in the $A_{2u(a)}$ mode.

side of the above equation, the first term arises from the cubic anharmonicity, while the second arises from the quartic one. Cubic anharmonicity gives rise to the dissipation of the vibrational energy by a three-phonon process diagrammatically shown in Fig. 6(b), while the quartic one gives rise to that by the four-phonon process shown in Fig. 6(c).

When the temperature T is not extremely high, Eq. (9) is not applicable. In order to obtain the damping constant at intermediate temperatures, Eq. (9) was generalized by assuming for convenience sake that the frequencies of phonons produced by a three-phonon process, ω_1 and ω_2, and those produced by a four-phonon process, ω'_1, ω'_2, and ω'_3, satisfy the relations $\omega_1 = \omega_2 = \tilde{\omega}_a = \frac{1}{2}\omega_j$ and $\omega'_1 = \omega'_2 = \omega'_3 = \tilde{\omega}_b = \frac{1}{3}\omega_j$, which led to the following equation:

$$\gamma_j = a[(e^{\hbar\tilde{\omega}_a/k_BT} - 1)^{-1} + \tfrac{1}{2}] + b\{[(e^{\hbar\tilde{\omega}_b/k_BT} - 1)^{-1} + \tfrac{1}{2}]^2 + \tfrac{1}{12}\}, \quad (10)$$

where k_B is Boltzmann's constant.

The observed temperature dependence of γ_j was interpreted by determining the factors a and b so that the curves given by Eq. (10) would show the best over-all fit to the observed values. The values of a and b in the best fit for the three modes are listed in Table III. The calculated curves of the cubic and quartic terms in Eq. (10) and of γ_j vs T for the $E_{u(3)}$, $A_{2u(a)}$, and $E_{u(b)}$ modes are represented in Figs. 7–9, which will be seen to be in excellent agreement with the plots of the observed values. From Table III, it will be found that the values of the ratio b/a amount to 0.04 in the $E_{u(3)}$, 0.08 in the $A_{2u(a)}$, and 1 in the $E_{u(b)}$ modes. A large value of b/a in the $E_{u(b)}$ mode is considered to be reasonable since the dissipation of the vibrational energy by a four-phonon process will be predominant because of the exceedingly high phonon energy of this mode. As seen in Figs. 7–9, the contribution of the quartic term becomes prominent with increasing temperatures.

The frequencies of the lattice vibration $E_{u(3)}$ and the molecular vibrations $A_{2u(a)}$ and $E_{u(b)}$ given in Table II show that the frequencies at the temperature T decrease slightly with increasing temperatures. By the theoretical treatment of lattice vibrations,[16] it is deduced that the frequency $\omega_j(T)$ of an anharmonic crystal is given as follows:

$$\omega_j(T) = \omega_j(0) + \delta\omega_j + \Delta\omega_j, \quad (11)$$

in which $\delta\omega_j$ represents the shift arising from the volume change of a primitive cell by thermal expansion and $\Delta\omega_j$ is that from the contribution of anharmonicity with increasing temperatures. Using the Grüneisen constant G, $\delta\omega_j$ of the one-phonon optic mode can be given as follows:

$$\delta\omega_j = \omega_j(0)[\exp(-G\textstyle\int_0^T \alpha_v dT) - 1]$$

$$\approx -\omega_j(0)[G\textstyle\int_0^T \alpha_v dT], \quad (12)$$

where α_v is a volume expansion coefficient which becomes $\alpha_\parallel + 2\alpha_\perp$ in the present case. Since $\omega_j(300\,^\circ\mathrm{K})$ obtained by a series of reflectivity measurements is most reliable, it is convenient to re-

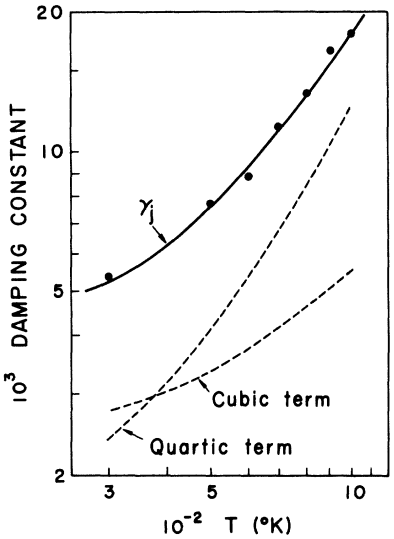

FIG. 9. Calculated curves of the cubic and quartic terms in Eq. (10) (dotted curves) and of γ_j (solid curve), and the plot of the observed values of γ_j in the $E_{u(b)}$ mode.

TABLE IV. Parameters used to calculate the frequency shift due to thermal expansion $[\delta\omega_j]^T_{300°\mathrm{K}}$ and the frequency shift due to anharmonicity $[\Delta\omega_j]^T_{300°\mathrm{K}}$, analyzed from the observed data. χ is the compressibility, C_v the specific heat, and G the Grüneisen constant.

T (°K)	$\int^T_{300°\mathrm{K}}(\alpha_\parallel + 2\alpha_\perp)\,dT$	χ (10^{-13} cm^2/dyn)	C_v (J/g)	G	$[\delta\omega_j]^T_{300°\mathrm{K}}$ (10^{14} sec^{-1})	$[\Delta\omega_j]^T_{300°\mathrm{K}}$ (10^{14} sec^{-1})
300	0	13.65	0.8196	0.5433	0	0
500	1.850×10^{-3}	14.65	1.045	0.4551	−0.0004	−0.008
600	3.831×10^{-3}	15.22	1.097	0.4365	−0.0009	−0.012
700	5.915×10^{-3}	15.86	1.137	0.4177	−0.0014	−0.017
800	8.085×10^{-3}	16.56	1.170	0.3970	−0.0018	−0.024
900	12.58×10^{-3}	17.35	1.200	0.3755	−0.0027	−0.029
1000	14.86×10^{-3}	18.24	1.227	0.3400	−0.0029	−0.037

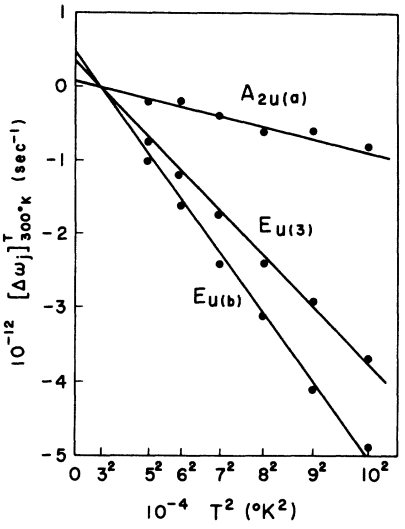

FIG. 10. Plots of the frequency shift due to anharmonicity $[\Delta\omega_j]^T_{300\,°K}$ in the $E_{u(3)}$, $A_{2u(a)}$, and $E_{u(b)}$ modes analyzed from the observed data.

write Eqs. (11) and (12) as follows:

$$[\omega_j(T)-\omega_j(300\,°\mathrm{K})]=[\delta\omega_j]^T_{300\,°\mathrm{K}}+[\Delta\omega_j]^T_{300\,°\mathrm{K}}, \quad (13)$$

$$[\delta\omega_j]^T_{300\,°\mathrm{K}}\approx-\omega_j(300\,°\mathrm{K})\,G\int^T_{300\,°\mathrm{K}}(\alpha_{\parallel}+2\alpha_{\perp})\,dT. \quad (14)$$

The numerical values of the integration in Eq. (14) for different values of T were obtained by applying Eqs. (8a) and (8b) up to 1000 °K, and are given in the second column of Table IV. The Grüneisen constant G was calculated by the relation $G=\alpha_v V_m/\chi C_v$, taking the molar volume $V_m=34.2\,\mathrm{cm}^3$ and using the values of the compressibility χ at various temperatures given in the third column[17] and those of the specific heat C_v given in the fourth column which were derived from the measured values of C_p.[18] The values of G obtained are listed in the fifth column, while those of $[\delta\omega_j]^T_{300\,°\mathrm{K}}$, in the sixth column. In the seventh column, the values of $[\Delta\omega_j]^T_{300\,°\mathrm{K}}$ obtained by subtracting $[\delta\omega_j]^T_{300\,°\mathrm{K}}$ from $[\omega_j(T)-\omega_j(300\,°\mathrm{K})]$ are given. They are plotted against T^2 in Fig. 10.

In the case of molecular vibrations, the carbon and oxygen ions concerned are situated in a plane perpendicular to the c axis to make a CO_3^{--} ion. The temperature change of the interionic separation within a CO_3^{--} ion, if ever, is considered to be too small to give rise to an appreciable frequency shift.[19] Therefore, the observed frequency shift $[\omega_j(T)-\omega_j(300\,°\mathrm{K})]$ should be ascribed solely to the shift due to the anharmonicity $[\Delta\omega_j]^T_{300\,°\mathrm{K}}$. In Fig. 10, the values of $[\Delta\omega_j]^T_{300\,°\mathrm{K}}$ of the $A_{2u(a)}$ and $E_{u(b)}$ modes are also plotted against T^2. It will be seen in this figure that the curves of the three modes show an excellent linearity. By extrapolating these curves down to $T=0$, the values of $[\Delta\omega_j]^T_0$ for the three modes were obtained and are listed in Table V.

It has been showed by Ipatova *et al.*[13,14] that the frequency shift $\Delta\omega_j(T)$ can be written as follows:

$$\Delta\omega_j(T)=\Delta\omega_j'(T)+\Delta\omega_j''(T), \quad (15)$$

where $\Delta\omega_j'(T)$ and $\Delta\omega_j''(T)$ are the frequency-independent and frequency-dependent parts of $\Delta\omega_j(T)$, which, in the high-temperature limit, have the following forms:

$$\Delta\omega_j'(T)=CT-DT^2, \quad (16a)$$

$$\Delta\omega_j''(T)=-C'T-D'T^2\,. \quad (16b)$$

In order to obtain the frequency shift at intermediate temperatures, these equations were generalized, which led to the following equations:

$$\Delta\omega_j'(T)=c\,[(e^{\hbar\tilde{\omega}_a/k_BT}-1)^{-1}+\tfrac{1}{2}] - d\,[(e^{\hbar\tilde{\omega}_b/k_BT}-1)^{-1}+\tfrac{1}{2}]^2, \quad (17a)$$

$$\Delta\omega_j''(T)=-c'\,[(e^{\hbar\tilde{\omega}_a/k_BT}-1)^{-1}+\tfrac{1}{2}] - d\,\{[(e^{\hbar\tilde{\omega}_b/k_BT}-1)^{-1}+\tfrac{1}{2}]^2+\tfrac{1}{12}\}, \quad (17b)$$

where c, d, c', and d' are positive constants. The first and second terms of the frequency-independent part $\Delta\omega_j'(T)$ arise from the processes diagrammatically shown in Figs. 6(a) and 6(d), while those of the frequency-dependent part $\Delta\omega_j''(T)$ arise from the processes shown in 6(b) and 6(c) which contribute to the damping constant. If the frequency shift, $[\Delta\omega]^T_0$ is governed by the frequency-dependent part, it would show that the temperature dependence is considerably different between the $E_{u(3)}$ and $E_{u(b)}$ modes with respect to the power of T, which, however, is not the present case. Therefore, it is conceivable that the frequency shift is mainly caused by the frequency-independent part. By taking $c=0$ and $d=0.91\times10^{11}$, 1.8×10^{11}, and 27×10^{11} sec^{-1} for the $E_{u(3)}$, $A_{2u(a)}$, and $E_{u(b)}$ modes, respectively, Eq. (17a) gives the curves of $[\Delta\omega_j']^T_0$ vs T represented in Figs. 11 and 12, which will

TABLE V. Frequency shift due to anharmonicity $[\Delta\omega_j]^T_0$, analyzed from the observed data in the $E_{u(3)}$, $A_{2u(a)}$, and $E_{u(b)}$ modes.

T (°K)	$E_{u(3)}$ $[\Delta\omega_j]^T_0$ (10^{11} sec^{-1})	$A_{2u(a)}$ $[\Delta\omega_j]^T_0$ (10^{11} sec^{-1})	$E_{u(b)}$ $[\Delta\omega_j]^T_0$ (10^{11} sec^{-1})
300	−4	−1	−5
500	−12	−3	−15
600	−16	−3	−21
700	−21	−5	−29
800	−28	−7	−36
900	−33	−7	−46
1000	−41	−9	−54

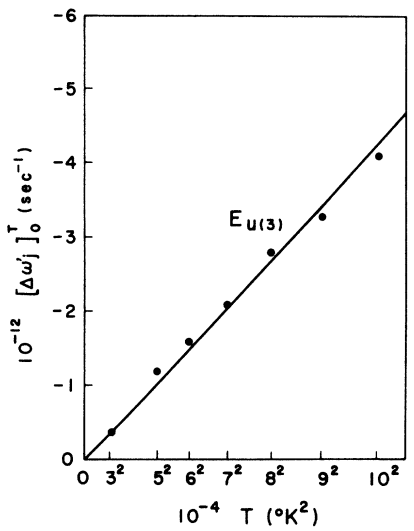

FIG. 11. Curve of the frequency shift due to anharmonicity $[\Delta\omega_j']_0^T$ given by Eq. (17a) and the plot of the values of $[\Delta\omega_j']_0^T$ analyzed from the observed data in the $E_{u(3)}$ mode.

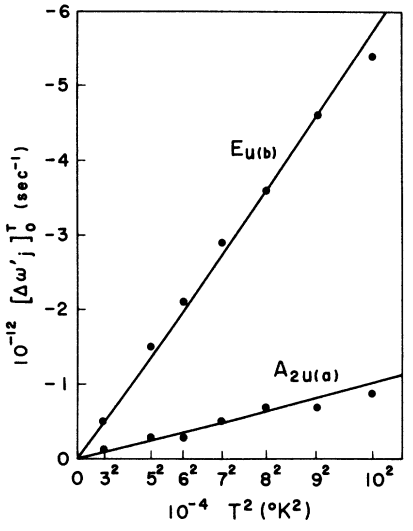

FIG. 12. Curves of the frequency shift due to anharmonicity $[\Delta\omega_j']_0^T$ given by Eq. (17a) and the plots of the values of $[\Delta\omega_j']_0^T$ analyzed from the observed data in the $A_{2u(a)}$ and $E_{u(b)}$ modes.

be seen to be in excellent agreement with the plots of the observed values. From these facts, it may safely be concluded that the contribution of quartic anharmonicity to the frequency shift predominates throughout the three modes.

In the above, the temperature dependence of the vibration parameters in one-phonon optic modes was interpreted by a theory consistent for lattice and molecular vibrations. For this problem, more information will be obtained by analyzing the observed change with temperature of summation bands in the near-infrared region, which, however, will be left to future investigations.

ACKNOWLEDGMENT

The authors wish to thank Dr. Mareo Ishigame for his helpful discussions.

*Present address: Department of Physics, Hirosaki University, Hirosaki, Japan.

[1]H. O. McMahon, J. Opt. Soc. Am. 40, 376 (1950).

[2]C. Shaefer and F. Matossi, *Das Ultrarote Spektrum* (Springer, Berlin, 1930), p. 356.

[3]R. S. Krishnan, Proc. Indian Acad. Sci. A22, 182 (1945).

[4]J. Louisfert, Compt. Rend. 241, 940 (1955); 248, 1150 (1959).

[5]J. Morandat and J. Lecomte, Compt. Rend. 263, 735 (1966).

[6]F. Matossi and V. Hohler, Z. Naturforsch. 22a, 1516 (1967).

[7]K. H. Hellwege, W. Lesch, M. Plihal, and G. Schaack, Z. Physik 232, 61 (1970).

[8]M. Born and M. Blackman, Z. Physik 82, 551 (1933).

[9]G. Heilmann, Z. Physik 152, 368 (1958).

[10]G. O. Jones, D. H. Martin, P. A. Mawer, and C. H. Perry, Proc. Roy. Soc. (London) A261, 10 (1961).

[11]A. D. B. Woods, B. N. Brockhouse, R. A. Cowley, and W. Cochran, Phys. Rev. 131, 1025 (1963).

[12]E. R. Cowley and R. A. Cowley, Proc. Roy. Soc. (London) A287, 259 (1965).

[13]R. F. Wallis, I. P. Ipatova, and A. A. Maradudin, Fiz. Tverd. Tela 8, 1064 (1966) [Sov. Phys. Solid State 8, 850 (1966)].

[14]I. P. Ipatova, A. A. Maradudin, and R. F. Wallis, Phys. Rev. 155, 882 (1967).

[15]K. V. K. Rao, S. V. N. Naidu, and K. S. Murthy, J. Phys. Chem. Solids 29, 245 (1968).

[16]S. S. Mitra, in *Optical Properties of Solids*, edited by S. Nudelman and S. S. Mitra (Plenum, New York, 1969), p. 388.

[17]D. P. Dandekar, J. Appl. Phys. 39, 3694 (1968).

Vol. IV, edited by K.-H. Hellwege and A. M. Hellewege (Springer, Berlin, 1967), part 6, p. 878.

[18]*Landolt-Börnstein Zahlenwerte und Funktioner*, Vol. IV, edited by K.-H. Hellweg and A. M. Hellweg (Springer, Berlin, 1967), p. 878.

[19]H. D. Megaw, Acta Cryst. A26, 235 (1970).